

Acoustic Array Biochip Combined with Allele-Specific PCR for Multiple Cancer Mutation Analysis in Tissue and Liquid Biopsy

Nikoletta Naoumi, Kleita Michaelidou, George Papadakis, Agapi E. Simaiaki, Román Fernández, Maria Calero, Antonio Arnau, Achilleas Tsortos, Sofia Agelaki, and Electra Gizeli*



Cite This: *ACS Sens.* 2022, 7, 495–503



Read Online

ACCESS |



Metrics & More



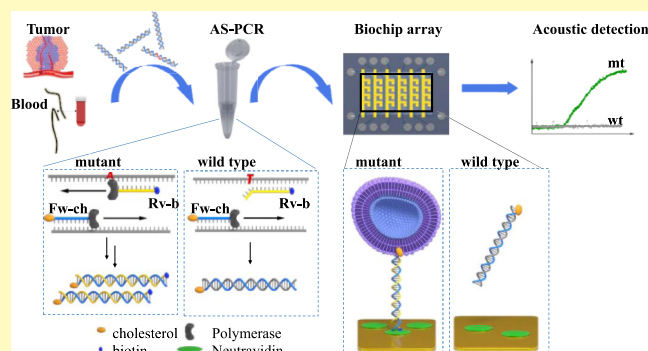
Article Recommendations



Supporting Information

ABSTRACT: Regular screening of point mutations is of importance to cancer management and treatment selection. Although techniques like next-generation sequencing and digital polymerase chain reaction (PCR) are available, these are lacking in speed, simplicity, and cost-effectiveness. The development of alternative methods that can detect the extremely low concentrations of the target mutation in a fast and cost-effective way presents an analytical and technological challenge. Here, an approach is presented where for the first time an allele-specific PCR (AS-PCR) is combined with a newly developed high fundamental frequency quartz crystal microbalance array as biosensor for the amplification and detection, respectively, of cancer point mutations. Increased sensitivity, compared to fluorescence detection of the AS-PCR amplicons, is achieved through energy dissipation measurement of acoustically “lossy” liposomes binding to surface-anchored dsDNA targets. The method, applied to the screening of *BRAF* V600E and *KRAS* G12D mutations in spiked-in samples, was shown to be able to detect 1 mutant copy of genomic DNA in an excess of 10^4 wild-type molecules, that is, with a mutant allele frequency (MAF) of 0.01%. Moreover, validation of tissue and plasma samples obtained from melanoma, colorectal, and lung cancer patients showed excellent agreement with Sanger sequencing and ddPCR; remarkably, the efficiency of this AS-PCR/acoustic methodology to detect mutations in real samples was demonstrated to be below 1% MAF. The combined high sensitivity and technology-readiness level of the methodology, together with the ability for multiple sample analysis (24 array biochip), cost-effectiveness, and compatibility with routine workflow, make this approach a promising tool for implementation in clinical oncology labs for tissue and liquid biopsy.

KEYWORDS: high fundamental frequency QCM, dissipation monitoring, liposomes acoustic amplification, *BRAF* V600E, *KRAS* G12D, molecular diagnostics, clinical oncology, companion diagnostics



Tumor tissue biopsy remains the gold standard method for cancer diagnosis and is an important source for routine molecular profiling of hotspot somatic mutations. However, conventional tissue biopsy has a number of limitations that stem from its invasive nature. In many cases, it is not feasible to perform tissue biopsy and the method is inappropriate for capturing intratumor heterogeneity, longitudinal profiling of cancer biomarkers, and monitoring of disease progression.^{1–3} Liquid biopsy is a promising noninvasive alternative that allows the study and characterization of different biomarkers such as cell-free DNA (cfDNA) fragments originating from tumor cells. Circulating tumor DNA (ctDNA) may carry the same genetic alterations as those of a primary tumor and thus, can serve as a valuable diagnostic and prognostic tool to select targeted therapies and monitor therapeutic response in real time.⁴ While liquid biopsy is simpler, faster, and more cost-effective than tissue biopsy, ctDNA detection poses an analytical challenge because it is present in very small

quantities (z/aM) and is highly fragmented, and mutants (mt) exist in samples with a background of abundant wild-type (wt) cfDNA, exhibiting a ratio of mt/wt or a mutant allele frequency (MAF: $\text{mt}/[\text{mt} + \text{wt}]$) of $<0.1\%$.⁵

Mutation analysis of ctDNA can be performed by next-generation sequencing (NGS) and polymerase chain reaction (PCR)-based methods.^{6,7} NGS has contributed considerably to clinical oncology during genotyping and the identification of novel mutations; however, it is restricted by the high cost, complexity, slow turnaround time (days), and need for dedicated bioinformatics facility. Real-time quantitative PCR

Received: October 22, 2021

Accepted: December 28, 2021

Published: January 24, 2022



(qPCR) is applied routinely to cancer molecular analysis during the enzymatic amplification of target mutations and fluorescent detection of produced amplicons; however, qPCR is not sufficiently sensitive (10–20%)⁴ toward the detection of known mutations.^{8,9} Variants of qPCR based on the use of allele-specific (AS) primers, such as the amplification refractory mutation system, exhibit an improved sensitivity (down to 0.1%) but depend on complex, multistep assays.^{10,11} Digital PCR (dPCR) methods, that is, BEAMing (beads, emulsion, amplification, magnetics) and ddPCR (droplet dPCR), can provide absolute quantification including the ratio of mt to wt DNA present in a sample. However, while both dPCR methods have very high sensitivities of 0.01 and 0.001%, respectively, they are highly complex, employing one or more PCR steps taking place in water–oil emulsions and followed by flow cytometry for the detection of two fluorescent probes; moreover, both require expensive instrumentation (>100 K euros).^{4,12}

Recently, DNA biosensors, including electrochemical,^{13–15} optical,^{16,17} or acoustic,^{18–21} have been reported as an alternative means for the detection of point mutations. Moreover, advances in biochips and nanotechnology have led to the development of enzymatic amplification-free protocols for ctDNA.^{7,22} Such examples include an electrochemical biochip combined with a clutch/clamp assay;²³ a plasmonic biosensor employing a peptide nucleic acid (PNA)-functionalized gold surface;²⁴ and a piezoelectric plate sensor combined with fluorescent reporter microspheres.²⁵ While the above works present elegant examples of the application of biosensors in PCR-free clinical diagnostics, achieving in one case a sensitivity similar to that of dPCR,²³ potential drawbacks include the (a) use of expensive PNA or locked nucleic acid (LNA) probes; (b) need for hybridization steps and temperature control; (c) laborious surface-activation and washing steps as well as nanoparticle synthesis and functionalization; and (d) low sensitivity, in cases when small volumes of the unpurified sample are used.

During the past decade, liquid biopsy has received tremendous attention; therefore, there is an urgent need for the development of diagnostic tools for immediate application in the clinic.²⁶ Inspired by the above, we developed a method for the detection of point mutations utilizing a novel high fundamental frequency quartz crystal microbalance (HFF-QCM) array device with energy dissipation monitoring allowing multisample analysis through the use of 24 resonators. The proposed methodology employs initially allele-specific PCR (AS-PCR) for the amplification of mt DNA targets carrying the *BRAF* V600E or *KRAS* G12D point mutation in a background of an excess of wt molecules. We focus on the *BRAF* and *KRAS* genes because they are two of the most prevalent druggable genetic mutations in some of the most common types of cancer.^{27,28} For the acoustic detection of the amplicons, we designed the assay so that the double-stranded DNA (dsDNA) products could be directly immobilized on the device surface, obviating the need for a hybridization step. Furthermore, we preferentially monitored the energy dissipation signal of the acoustic wave instead of the frequency one and employed liposomes as acoustic signal enhancers. This approach was shown to improve the detection capability of the assay and detect down to 1 mt copy in the initial sample in the presence of 10⁴ wt DNAs. The clinical validity of the assay was further demonstrated during the successful detection of *BRAF* and *KRAS* point mutations in colorectal, lung, and melanoma

cancer patients' tissue and plasma samples. Results indicate the excellent sensitivity of the method, higher than that obtained with qPCR and comparable to dPCR but through a simpler and less expensive methodology of the latter.

EXPERIMENTAL SECTION

Acoustic Array and QCM Sensor. A newly developed platform was used to monitor the 150 MHz HFF-QCM acoustic array (both by AWS, S.L. Paterna, Spain). 35 MHz QCM sensors (7th overtone) (AWS, S.L. Paterna, Spain) were monitored using the Q-Sense E4 instrument (Biolin Scientific, Sweden) (see also S1).

Acoustic Detection of b-BSA and NAV. NeutrAvidin (NAV-Invitrogen) (0.2 mg/mL) and biotinylated bovine serum albumin (b-BSA) (0.2 mg/mL) diluted in PBS pH = 7.4 (Sigma-Aldrich) were applied on the device surface; 0.05 mg/mL of NAV was further applied on the b-BSA layer. b-BSA was prepared as described in S2. The working volumes of the HFF array (150 MHz) and QCM (35 MHz) devices were 60 and 200 μ L, respectively.

Liposome Preparation. POPC liposomes (1-palmitoyl-2-oleoyl-*sn*-glycero-3-phosphocholine) from Avanti Polar Lipids (Alabaster, AL, U.S.A.) were prepared as described before.³⁹ Briefly, an initial solution of 2 mg lipid/mL was prepared in PBS buffer and extruded through a polycarbonate filter; the filtered solution was stored (up to 3 days) and was used at a dilution of 10 times for the sensing experiments. The extrusion process results in rather narrow size distributions with average diameters near those of the employed filter pore (here 200 nm).^{29–31} Liposome polydispersity effects on the recorded QCM signal are of minor importance.³² Nevertheless, care was taken to use, as much as possible, the same particle batch (preparation); the resulting reproducibility of the acoustic signal in our experiments was very good (standard deviation \sim 15%, see Table in Figure 2D).

HFF-QCM Detection of dsDNA and Liposomes. Biotinylated at 5'-end dsDNA (b-DNA) fragments of 21, 50, 75, and 157 bp were prepared according to ref 39 and applied (60 μ L of 83 or 500 nM) to a NAV precoated array. Then, 100 POPC were added for DNA detection.

Acoustic Analysis of AS-PCR. A sample of 2.5 μ L or 8 μ L of the *BRAF* or *KRAS* AS-PCR, respectively, diluted in a total volume of 20 μ L, was loaded on the 150 MHz HFF-QCM array (flow rate: 14 μ L/min), which was precoated with b-BSA/NAV. Similarly, 2.5 or 10 μ L of the *BRAF* or *KRAS* AS-PCR, diluted in a total volume of 125 μ L, was applied to the 35 MHz QCM device (25 μ L/min). In both cases, a suspension of POPC liposomes was added at a volume of 100 μ L (150 MHz) and 500 μ L (35 MHz).

***BRAF* V600E and *KRAS* G12D AS-PCR.** For *BRAF* V600E, KAPA2G Fast HotStart ReadyMix (KAPABIOSYSREMS) was mixed with 5 pmol of the AS-biotinylated reverse (Rv) primer and 5 pmol of the cholesterol-modified forward (Fw) primer in a total volume of 10 μ L. For *KRAS* G12D, 10 pmol of the mutation-specific biotinylated Fw primer, 10 pmol of the cholesterol-modified Rv primer, and 1 μ L of 20X SYBR Green I Nucleic Acid Stain (Lonza) were mixed with KAPA2G Fast HotStart ReadyMix in a total of 20 μ L (see also S3 and Table S1).

Sample Collection. 21 formalin-fixed paraffin-embedded (FFPE) tissue and 20 plasma samples were obtained from patients with various cancer types at the University Hospital of Heraklion. The research protocol was approved by the Institutional Ethics Committee of the University Hospital, and all patients provided written informed consent to participate in the study.

Sanger Sequencing and ddPCR. Genomic DNA from FFPE tissues was amplified by PCR using specific primer pairs for *KRAS* exon 2 and *BRAF* exon 15 (Table S1). Sequencing reactions were performed using the Big Dye terminator V3.1 cycle sequencing kit (Applied Biosystems) according to the manufacturer's protocol. The products were then assessed by capillary electrophoresis on an ABI3130 system, and results were analyzed using Sequencing Analysis software v5.4 (Applied Biosystems). cfDNA was isolated from 2 mL of plasma for each sample via the QIAamp circulating nucleic acid kit

(Qiagen). ddPCR was performed using the QX200 Droplet Digital PCR System (Bio-Rad), as previously described,³³ and the KRAS G12/G13 and the BRAF V600 Screening Multiplex Kits (Bio-Rad) (see also S4).

RESULTS AND DISCUSSION

Concept of Combined AS-PCR/Acoustic Detection.

The main objective of this work was to design a methodology for liquid and tissue biopsy that could exhibit the high sensitivity of dPCR (BEAMing and ddPCR) using a less cumbersome and more cost-effective method. The protocol we developed involves the specific amplification of the point mutation via AS-PCR followed by acoustic detection using a novel array biochip device and a two-step assay. The basic principle of the methodology is presented in Figure 1A,B.

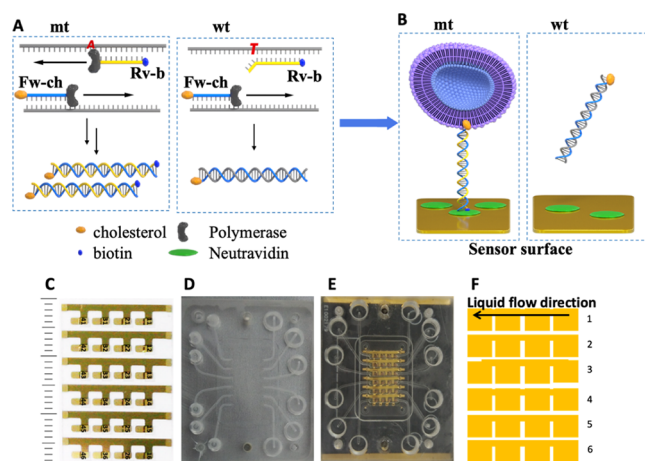


Figure 1. (A) Schematic illustration of the AS-PCR regarding the primer design and annealing step: the reverse (Rv: yellow) and forward (Fw: blue) primers are hybridized to the denatured single-stranded BRAF V600E point-mutation targets (gray); note that a double-labeled (biotin and cholesterol) amplicon is produced only in the case of the mt DNA as opposed to a single-labeled DNA (cholesterol) in the case of the wt, as a result of the use of labeled primers (biotinylated-Rv and cholesterol-Fw). (B) Acoustic detection during binding of the biotinylated amplified mt target to the NAV-modified surface followed by liposome's anchoring to the cholesterol probe also attached to the amplified mt target; (C) acoustic array consists of 24 HFF-QCM sensors arranged in six lines of four sensors; (D) PDMS flow cell alone and (E) integrated with the array/PCB board; (F) schematic representation of the liquid flow along the six lines and over the four sensors.

PCR is based on three simple steps required for any DNA synthesis, that is, (1) denaturation of the template into single strands; (2) annealing of primers to each original strand for new strand synthesis; and (3) extension of the new DNA strands from the primers. A critical part of a successful PCR is the design of the primers based on the optimization of factors such as their length, melting temperature, % of guanine-cytosine content, and lack of complementary regions between themselves.³⁴ Here, for the specific amplification of the mutant allele with AS-PCR, we wanted both sets of primers to create a short PCR product of less than 90 bp in order to target the highly fragmented ctDNA (90–150 bp).³⁵ The set of primers used from the literature¹¹ include a Fw primer that amplifies both the mt and wt sequences due to full complementarity with both strands, while the Rv one amplifies only the mt target; this is due to the Rv design which has the AS nucleotide

for the mt target at the end of the 3'-end, resulting only in full match and efficient amplification of the mt target. In this application and for the sake of the downstream acoustic analysis, the Fw primer is modified with a cholesterol in its 5'-end and the Rv primer with a biotin (Figure 1A). Following amplification, DNA fragments of 89 bp employing both a biotin and a cholesterol molecule in the case of the mt target or only a cholesterol molecule in the case of the wt target are produced. The AS-PCR is then loaded directly on the NAV-modified acoustic biochip without prior purification, where only the mt DNA-amplicons which carry the biotin are immobilized. In order to achieve the clinically relevant detection limits of few copies of the mt target in the presence of larger amounts of the wt, ultrasensitive detection is necessary, even after AS-PCR. This becomes even more significant if detection occurs using the crude AS-PCR cocktail where issues of nonspecific binding become a concern. For this reason, in a follow-up step, a solution of POPC liposomes is injected and captured by the immobilized products via the cholesterol-end of the mt amplified products (Figure 1B). Liposomes act as dissipation signal-enhancers causing large changes in the acoustic signal leading to the detection of immobilized DNA. This strategy has been shown by our group as well as others to be suitable for the acoustic detection of recombinase polymerase amplification products;³⁶ the frequency signal has also been used in combination with liposomes to detect single-base mismatches.^{37–39}

Acoustic Array Biochip for Multiple Sample Analysis.

The HFF resonator array used in this work includes 24 miniaturized crystals integrated monolithically to a single substrate, in a layout of six rows with four resonators/row (Figure 1C). The HFF-QCM array chip is ideal for high-throughput analysis⁴⁰ and low-volume biosensing applications. Because the array is very small and fragile for direct handling during experiments, it was mounted on a printed circuit board (PCB); the latter also provides mechanical, electrical, and thermal interface between the acoustic wave device and the recording instrument. A gasket and a cell have been developed and integrated with the PCB + array assembly (Figure 1D,E). The flow cell device seals the microsensors individually, so that it is possible to flow liquid in the desired direction over the sensor top surface without affecting the array electrical connections placed on the bottom surface or interfere with the different lines of sensors. During experiment, the liquid moves sequentially on each of the four sensors in the same row (Figure 1F), running from the input to the output. Each crystal has 0.3114 mm² active surface area and 1.5 μ L volume above the sensor. With the current flow setup, six samples can be analyzed in a semiparallel way with the possibility to perform four tests per sample. More information on the array can be found in ref 41.

Performance Evaluation of the Biochip Array. The principle of operation of the HFF-QCM resonator is the same as that of a typical acoustic device; briefly, the presence of an analyte on the sensor surface affects the propagation characteristics of the acoustic wave, that is, its velocity and amplitude, which in turn are expressed as changes in frequency (ΔF) and energy dissipation (ΔD). ΔF correlates with the amount of the deposited mass on the sensor;⁴² ΔD and ($\Delta D/\Delta F$) correlate, among other things, with the viscoelastic properties of the surface-attached layer and hydrodynamic properties^{43–45} or conformation^{46–49} of discretely-bound molecules. We first analyzed the device responses during the

adsorption of proteins as well as the detection of dsDNA and compared them to the response of the standard 35 MHz QCM-D. Specifically, the physisorption of NAv and b-BSA protein directly on gold was first recorded as well as the subsequent binding of NAv on a preadsorbed layer of b-BSA. In all cases, ΔF and ΔD were measured at equilibrium and at surface saturation. Figure 2A,B shows that the relative signal

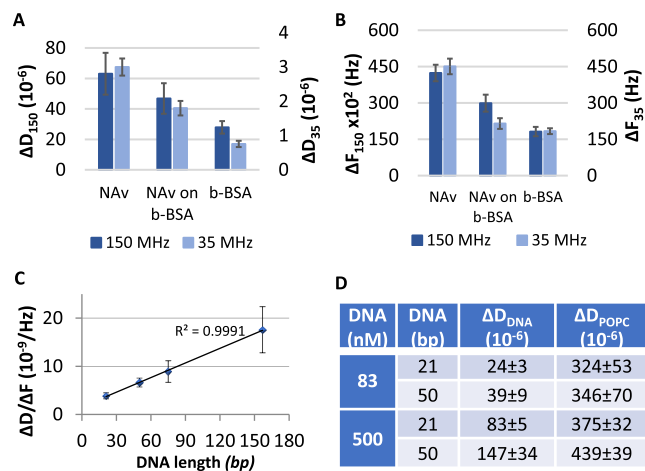


Figure 2. Comparison of ΔD (A) and ΔF values (B) of NAv and b-BSA adsorption as well as NAv binding to preadsorbed b-BSA on the 150 and 35 MHz sensors; (C) acoustic ratio ($\Delta D/\Delta F$) as a function of the length of b-DNA attached on a NAv-modified surface; (D) table of ΔD values at saturation obtained with the 150 MHz HFF-QCM during the binding of DNA (83 and 500 nM) followed by the addition of liposomes (200 nm).

responses of all three proteins upon absorption/binding to the surface is the same for both devices. Moreover, the array biochip was tested and found to give the expected linear relationship between the DNA length and the acoustic ratio ($\Delta D/\Delta F$) during the binding of b-DNA molecules to a NAv-covered surface through a single point (Figure 2C).^{46,48}

The protocol we developed for the detection of cancer point mutations in crude samples includes a step of amplification through liposomes; for this reason, we further monitored the binding of 200 nm diameter POPC liposomes on dsDNA in buffer. We tested two different lengths of DNA, that is, 21 and 50 bp, carrying a biotin at their 5'-end for immobilization to the surface and a cholesterol at their 3'-end for the binding of liposomes. ΔD values measured with the 150 MHz QCM array biochip during liposome attachment gave a higher dissipation value when liposomes were bound to the longer DNA (Figure 2D), in agreement with previous studies.³⁹ Overall, the successful detection of proteins, DNA, and liposomes with the 150 MHz acoustic array demonstrate the suitability of the new system for subsequent application for the development of clinical biology assays.

Analytical Performance of the AS-PCR/Acoustic Assay for the Detection of Point Mutations Using Genomic DNA. (A) *BRAF V600E*. To determine the limit of detection (LOD) and sensitivity of the assay, mt genomic DNA carrying the *BRAF V600E* point mutation was mixed with wt DNA in a range from 0.01% to 10% (i.e., from 1:10⁴ to 1:10 mt/wt). The mt/wt dilutions as well as the 100% (10⁴ copies) wt genomic DNA (control) were subjected to 55 cycles of AS-PCR (1 h 40 min) followed by acoustic detection on the biochip array (10 min). For the immobilization of the

biotinylated mt target, we used a surface premodified with b-BSA/NAv which was shown in our lab to have a high stability in the presence of a crude sample (data not shown).

Initially, we investigated whether the ΔF and ΔD signals obtained from the direct detection of the immobilization of the AS-PCR products on the b-BSA/NAv-surface could differentiate between the mt and wt reactions. Results indicated poor discrimination between the two (Figure S1). We attribute this response to the nonspecific adsorption of components in the PCR cocktail (e.g., primer dimers, DNA polymerase, etc.) resulting in a background signal overshadowing the specific binding of the biotinylated amplicons. For this reason, we employed a second step, where liposomes were used as signal amplifiers upon binding at the 5' cholesterol present at the mt amplicon. The real-time binding of the liposomes to the AS-PCR modified surface was specific, giving nearly zero dissipation change in the absence of the mt target (Figure 3A). Figure 3B summarizes the average dissipation values

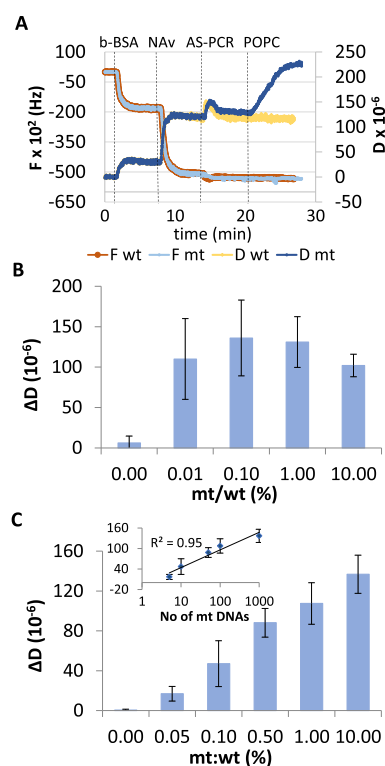


Figure 3. Results obtained with the HFF-QCM (150 MHz) using spiked-in genomic DNA: (A) Real-time acoustic detection of the *BRAF V600E* mutation (10 copies) together with a control sample (10⁴ wt DNAs); (B) Recorded acoustic values (saturation) during the detection of the *BRAF V600E* mixed with wt DNA in a range from 0 to 10%; (C) as in (B) for the *KRAS G12D*. The inset shows the linear curve relationship ($R^2 = 0.95$) of the obtained ΔD values when plotted vs the number of mt molecules in logarithmic scale. The 0.00% corresponds to the control (10⁴ wt molecules).

recorded at the liposome step for all the mt/wt dilutions; based on this data, the sensitivity and LOD for the detection of *BRAF V600E* is 0.01% mt/wt copies and 1 copy, respectively. For the same samples, the frequency response was not able to reliably discriminate positive from negative samples (Figure S2). This is in agreement with previous works, where the dissipation signal was proven to be more sensitive than frequency for

ultrasensitive detection of DNA (fmol) via liposomes as signal amplifiers.^{36,39}

Figure 3B shows that the assay provides only qualitative results because it can differentiate between the presence or absence of the mutation but cannot distinguish between the various mt/wt ratios. This is attributed to the fact that the AS-PCR had reached a plateau after the 55 cycles employed in this assay.

(B) *KRAS G12D*. The combined AS-PCR/acoustic methodology was further applied to the detection of the *KRAS G12D* mutation. For this assay, a slightly modified version of Figure 1A was employed: here, the Rv primer was modified by a cholesterol and designed to amplify both the mt and wt targets, while the Fw was biotinylated and was specific for the mutant allele. Similarly to the *BRAF*, the analytical performance of the assay was investigated by mixing genomic DNA carrying the *KRAS G12D* point mutation with wt DNA at gradually decreasing ratios ranging from 0.05 to 10%. The mt/wt dilutions and control of 100% (10^4 copies) wt genomic DNA were subjected first to real-time AS-PCR; this was in order to determine the number of cycles needed for all the samples to be at the range of the exponential-to-early-plateau phase of the PCR relative to their initial mt DNA input. Based on these results (Figure S3), a modified protocol for the AS-PCR including 45 cycles (1 h) was established and used for the *KRAS* detection. For the acoustic analysis, liposome addition on the biochip array preloaded with the mt/wt solutions allowed the clear distinction between the mt from the wt samples (Figure 3C). Moreover, the ΔD values obtained upon liposome addition were analogous to the initial mt/wt ratio; the linear relationship obtained between ΔD and the absolute number (logarithmic) of mt molecules ($R^2 = 0.95$) indicates that the method is quantitative (Figure 3C inset), with a sensitivity and LOD of 0.05% and 5 molecules, respectively. Regarding frequency change, the response was not as sensitive as the dissipation, giving a reliable discrimination only at the level of the 10% mt/wt (Figure S4).

A notable difference to the *BRAF* analysis was that the ΔD measurement obtained from the direct binding of the AS-PCR products on the b-BSA/Nav-coated surface could discriminate to some extent the mt/wt ratios from the wt, although the error bars were very large (Figure S5). This is attributed to the higher volume used for the *KRAS* AS-PCR as opposed to the *BRAF* one ($20 \mu\text{L}$ vs $10 \mu\text{L}$) and for loading on the HFF-QCM sensor surface ($8 \mu\text{L}$ vs $2.5 \mu\text{L}$). Moreover, the reduction of the AS-PCR cycles to 45 may have also resulted in fewer byproducts and lower nonspecific binding. The above results indicate that optimized assays can provide ultrasensitive, specific, and quantitative information through acoustic measurement of the dissipation signal.

Effect of the Operating Frequency. To evaluate the efficiency of the 150 MHz acoustic biochip array toward the analysis of cancer point mutations we used the standard 35 MHz QCM sensor to perform the same assays and compare results. Differences between the two devices would include the penetration depth inside the sensed solution (43 nm for the 150 MHz and 90 nm for the 35 MHz) and the size of the two QCM-devices, geometry of the flow cell and applied flow rate; the latter can affect the amount of the immobilized target.

Based on Figure 4A,B, we conclude that the two devices give the same dissipation response and LOD toward the detection of all tested mt/wt AS-PCR samples. Moreover, the 35 MHz device also failed to detect the *BRAF* samples upon their direct

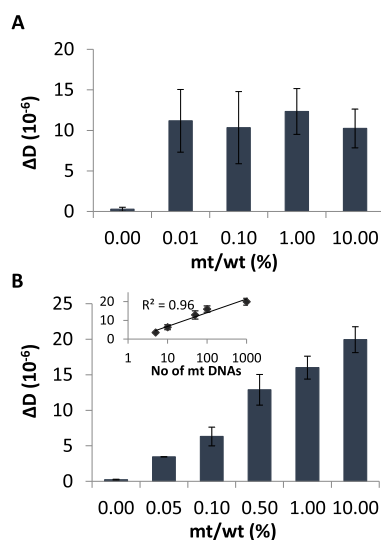


Figure 4. Results obtained with the QCM (35 MHz) using spiked-in genomic DNA: (A) obtained acoustic values (saturation) during the detection of the *BRAF V600E* mixed with wt DNA in a range from 0 to 10%. (B) As in (A) for the *KRAS G12D*. The inset shows the linear curve relationship ($R^2 = 0.96$) of the obtained ΔD values when plotted vs the number of mt molecules in logarithmic scale. The 0.00% corresponds to the control (10^4 wt molecules).

loading on the b-BSA/Nav coated sensor (Figure S6) while some discrimination capability mainly through the ΔD signal was recorded in the case of *KRAS* AS-PCR samples (Figure S7).

Clinical Validation during the Analysis of *BRAF* and *KRAS* Mutations in Tissue Samples. The final goal of this work was to assess the capability of the method to detect ctDNA carrying point mutations in patients' samples. For this reason, we evaluated the ability of the combined AS-PCR/acoustic method to detect *BRAF V600E* and *KRAS G12D* mutant alleles in clinical FFPE tissue samples based on the protocols described before. Regarding the *BRAF V600E* mutation, 11 samples collected from lung (L), melanoma (MEL), and colorectal cancer (CRC) patients' tissues as well as healthy individuals were tested. Of the above, six were positive and five negative, as identified by Sanger sequencing and ddPCR. For the *KRAS* mutation, 10 samples were tested also derived from patients and healthy individuals. Results obtained from AS-PCR/acoustic detection are summarized in Figure 5. ddPCR was further used to quantify the absolute number of mt and wt copies present in each sample and calculate the % of MAF. A Table summarizing results from all three techniques (i.e., Sanger, ddPCR, and acoustic) is provided in the Supporting Information (Table S2).

Based on Figure 5 and Table S2, no false positives or false negatives were recorded indicating 100% sensitivity and specificity for both targets. Moreover, all wt samples gave a zero response, indicating the power of the proposed acoustic methodology to discriminate (positive/negative result) between malignant and benign tissues. Finally, the frequency measurement failed to discriminate malignant from healthy tissue samples (data not shown).

Clinical Validation during *KRAS* and *BRAF* Mutation Detection in Patients' Plasma Samples. The method was further evaluated for the detection of ctDNA targets carrying the *BRAF V600E* or *KRAS G12D* mutation using cfDNA derived from patients' plasma samples, that is, during liquid

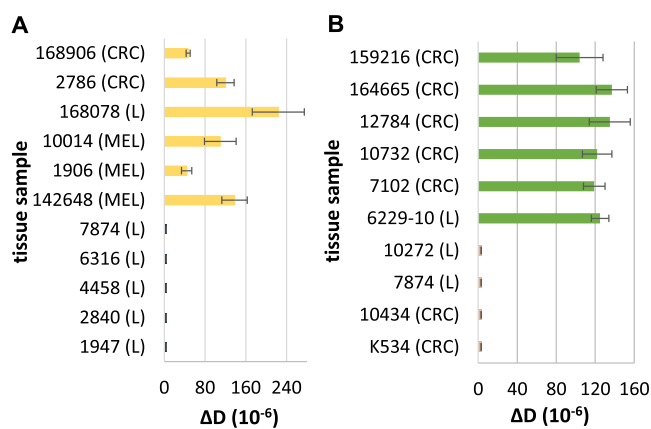


Figure 5. Validation of the methodology during tissue biopsy: (A) Comparison of ΔD values obtained from the analysis of patients' *BRAF* wt and *BRAF* V600E tissue samples by AS-PCR and acoustic detection (150 MHz). (B) Same as in (A) for *KRAS* wt and *KRAS* G12D samples. Yellow and green bars represent the *BRAF* V600E and *KRAS* G12D samples, respectively; all other samples refer to wt *BRAF* (1947, 2840, 4458, 6316, and 7874) and *KRAS* (K534, 10434, 7874, and 10272) which produced zero acoustic response upon liposome addition. (MEL-Melanoma; L-lung; CRC-Colorectal).

biopsy. For this, 10 plasma samples identified as *BRAF* V600E or *BRAF* wt by ddPCR were subjected to AS-PCR followed by acoustic detection; for these experiments, 50 cycles (1 1/2 h) of AS-PCR were used instead of 55, following further optimization of the protocol. In contrast to results obtained with tissue samples, in the case of plasma a change in ΔD was detected for the wt specimens, although much lower than that obtained for positive samples. Gel electrophoresis, performed to identify the source of the background signal, showed a high degree of byproducts even after 50 PCR cycles, possibly due to the presence of cholesterol-primer aggregation. To define the cutoff value above which ΔD change would be considered as an indication of a positive sample, we calculated the mean ΔD value from all wt samples (healthy) plus three standard deviations;²³ this value was set at $\Delta D 80 \times 10^{-6}$. Based on the above and results presented in Figure 6A, we concluded that all samples carrying the *BRAF* V600E point mutation were correctly identified with our method as positive and negative when compared with ddPCR results (Table S3). Statistical analysis verified that the mt/wt populations were significantly different ($p < 0.001$). Regarding the *KRAS* G12D mutation analysis, 10 samples identified as *KRAS* G12D or *KRAS* wt by ddPCR were blindly tested by the AS-PCR/acoustic detection, as well. According to Figure 6B and Table S3, the combined AS-PCR/acoustic method provided results in full agreement with the ddPCR. Note that, two samples corresponding to 27 (11MEL) and 19 (1797L) *BRAF* and *KRAS* mutant copies, respectively, and a MAF value of $<1\%$ were clearly identified as positive by the acoustic method (Table S3). Finally, frequency response was only able to discriminate plasma samples bearing the *KRAS* mutation but not the *BRAF* one (Figure S8).

Comparison of the Combined AS-PCR/Acoustic Method to Current State-of-the-Art for Liquid Biopsy. AS-PCR has been used extensively for the detection of mutations in serum and plasma. So far, both the traditional assay and its variants^{10,11,50–53} have limited analytical sensitivity (in the range of 0.1–2%), affecting their broad clinical use. Moreover, alternative PCR assays employing PNA⁵⁴ or LNA-molecules⁵⁵ require specifically designed and

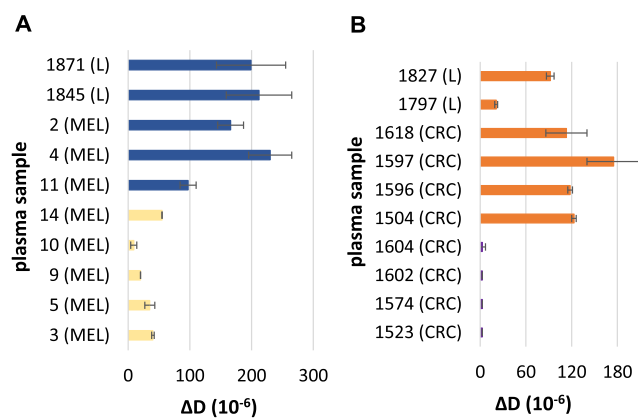


Figure 6. Validation of the methodology during liquid biopsy: (A) Comparison of ΔD values obtained from the analysis of patients' *BRAF* wt and *BRAF* V600E plasma samples by AS-PCR and acoustic detection (150 MHz). Yellow and blue columns correspond to *BRAF* wt and *BRAF* V600E samples, respectively. (B) Same as in (A) for *KRAS* wt and *KRAS* G12D samples (orange); note that in this case all wt samples gave a nearly zero acoustic response. (MEL-Melanoma; L-lung; CRC-Colorectal).

expensive probes and more cumbersome and time-consuming steps without significantly increasing the sensitivity (0.1%). In all the above assays, detection takes place using fluorescent probes. The acoustic detection of the AS-PCR amplicons seems to be a promising alternative reaching a detection capability of 0.01% mutant alleles without increase in the complexity of the assay. We attribute the enhanced sensitivity of the acoustic methodology to the simple two-step assay employed, that is, first the direct immobilization of the amplicons on the device surface followed by acoustic signal-enhancement by liposomes. Desirable features of the proposed method are the use of double-labeled primers allowing the direct binding of dsDNA on the device bypassing the need for denaturation and surface hybridization as well as the high sensitivity of the dissipation signal which can detect fmol of target DNA.³⁹

Currently, one of the gold standards in a clinical oncology lab is the use of the qPCR-based COBAS mutation test; the method designed for tissue (*KRAS*, *EGFR* mutations) and liquid (*EGFR*) biopsy allows simultaneous detection of FFPE tissue and plasma samples within 8 and 4 h respectively and detects $\geq 5\%$ mutant allele copies in a background of wild-type DNA. Our proposed technique outperforms the above commercially available method in terms of both sensitivity (0.01–0.05%) and total analysis time (<5 and <3 h for tissue and plasma, respectively). However, the COBAS test offers the ability to detect a panel of mutations (19 *KRAS* and 42 *EGFR*) simultaneously. With the current acoustic biochip design, six samples can be detected per array (giving four readings per sample). Employing a new flow-cell design with the current array to test 8 (3 readings/sample) or 16 (2 readings/sample) mutations can improve multiple analysis. In addition, given the low cost of the biochip array ($<1\%$ for large scale production), two or three array biochips could be used in parallel, without significantly increasing the complexity and size of the instrumentation.

Compared to the dPCR, our technique is faster and more affordable but cannot provide absolute quantification. Our method is also more cost-effective because we use a standard thermocycler (<2.6 K€) and the acoustic platform (<10 K),

both an order of magnitude less expensive than a dPCR machine (110 K€). The development of a single platform integrating a thermocycling unit with acoustic detection is a feasible next step.

CONCLUSIONS

In this work, we report the fast and ultrasensitive detection of AS-PCR products using a new acoustic array biochip and a two-step detection assay employing liposomes for signal amplification. Specifically, we use the above methodology for the amplification and acoustic detection of *BRAF* V600E and *KRAS* G12D point mutations from patients' tissue and plasma samples. Based on our results, the dissipation signal emerges as a measurement of superior analytical capability than the widely used frequency one. AS-PCR was chosen for amplification due to the method's good sensitivity and already wide applicability on a routine basis with fluorescent detection. Combining AS-PCR with acoustic detection (ΔD) we achieved an improved, excellent sensitivity (0.01–0.05%), comparable to that of the best available method, that is, dPCR, but for a fraction of the cost and in a much faster manner. Together with its high technology-readiness level, the above results suggest the suitability of the method for clinical use in an oncology lab for both tissue and liquid biopsy.

ASSOCIATED CONTENT

Supporting Information

The Supporting Information is available free of charge at <https://pubs.acs.org/doi/10.1021/acssensors.1c02245>.

Further technical and analytical details on devices and assays, respectively; frequency and dissipation data during direct detection of target-DNA (no liposomes); real-time PCR curves; and the frequency response obtained during testing of clinical samples; the presented work has been uploaded at the bioRxiv preprint open access repository (PDF)

AUTHOR INFORMATION

Corresponding Author

Electra Gizeli – Department of Biology, University of Crete, Heraklion 70013, Greece; Institute of Molecular Biology and Biotechnology-FORTH, Heraklion 70013, Greece; orcid.org/0000-0002-3598-5984; Email: gizeli@imbb.forth.gr

Authors

Nikoletta Naoumi – Department of Biology, University of Crete, Heraklion 70013, Greece; Institute of Molecular Biology and Biotechnology-FORTH, Heraklion 70013, Greece

Kleita Michaelidou – Laboratory of Translational Oncology, School of Medicine, University of Crete, Heraklion 70013 Crete, Greece

George Papadakis – Institute of Molecular Biology and Biotechnology-FORTH, Heraklion 70013, Greece

Agapi E. Simaiaki – Department of Biology, University of Crete, Heraklion 70013, Greece

Román Fernández – Advanced Wave Sensors S. L., Paterna 46988, Spain; Centro de Investigación e Innovación en Bioingeniería, Universitat Politècnica de València, Valencia 46022, Spain

Maria Calero – Centro de Investigación e Innovación en Bioingeniería, Universitat Politècnica de València, Valencia 46022, Spain

Antonio Arnau – Advanced Wave Sensors S. L., Paterna 46988, Spain; Centro de Investigación e Innovación en Bioingeniería, Universitat Politècnica de València, Valencia 46022, Spain

Achilleas Tsortos – Institute of Molecular Biology and Biotechnology-FORTH, Heraklion 70013, Greece

Sofia Agelaki – Laboratory of Translational Oncology, School of Medicine, University of Crete, Heraklion 70013 Crete, Greece; Department of Medical Oncology, University General Hospital of Heraklion, Crete 71500, Greece

Complete contact information is available at:

<https://pubs.acs.org/10.1021/acssensors.1c02245>

Notes

The authors declare the following competing financial interest(s): Authors EG, AT, GP, RF and AA participate in a spin off company (AWSensors Diagnostics) created with the aim to promote acoustic devices and technologies to healthcare application including cancer diagnosis.

Manuscript preprint previously deposited to BioRxiv at <https://www.biorxiv.org/content/10.1101/2021.09.16.460590v1>.

ACKNOWLEDGMENTS

This work was supported by the European Union's Horizon H2020-FETOPEN-1-2016-2017 under grant agreement no. 737212 (CATCH-U-DNA).

REFERENCES

- Heitzer, E.; Haque, I. S.; Roberts, C. E. S.; Speicher, M. R. Current and future perspectives of liquid biopsies in genomics-driven oncology. *Nat. Rev. Genet.* **2019**, *20*, 71–88.
- Han, X.; Wang, J.; Sun, Y. Circulating Tumor DNA as Biomarkers for Cancer Detection. *Genomics, Proteomics Bioinf.* **2017**, *15*, 59–72.
- Parikh, A. R.; Leshchiner, I.; Elagina, L.; Goyal, L.; Levovitz, C.; Siravegna, G.; Livitz, D.; Rhrissorakrai, K.; Martin, E. E.; Van Seventer, E. E.; et al. Liquid versus tissue biopsy for detecting acquired resistance and tumor heterogeneity in gastrointestinal cancers. *Nat. Med.* **2019**, *25*, 1415–1421.
- Soda, N.; Rehm, B. H. A.; Sonar, P.; Nguyen, N.-T.; Shiddiky, M. J. A. Advanced liquid biopsy technologies for circulating biomarker detection. *J. Mater. Chem. B* **2019**, *7*, 6670–6704.
- Crowley, E.; Di Nicolantonio, F.; Loupakis, F.; Bardelli, A. Liquid biopsy: Monitoring cancer-genetics in the blood. *Nat. Rev. Clin. Oncol.* **2013**, *10*, 472–484.
- Elazezy, M.; Joosse, S. A. Techniques of using circulating tumor DNA as a liquid biopsy component in cancer management. *Comput. Struct. Biotechnol. J.* **2018**, *16*, 370–378.
- Gorgannezhad, L.; Umer, M.; Islam, M. N.; Nguyen, N.-T.; Shiddiky, M. J. A. Circulating tumor DNA and liquid biopsy: Opportunities, challenges, and recent advances in detection technologies. *Lab Chip* **2018**, *18*, 1174–1196.
- Acinas, S. G.; Sarma-Rupavtarm, R.; Klepac-Ceraj, V.; Polz, M. F. PCR-induced sequence artifacts and bias: Insights from comparison of two 16s rRNA clone libraries constructed from the same sample. *Appl. Environ. Microbiol.* **2005**, *71*, 8966–8969.
- Kanagawa, T. Bias and Artifacts in Multitemplate Polymerase Chain Reactions(PCR). *J. Biosci. Bioeng.* **2003**, *96*, 317–323.
- Lang, A. H.; Drexel, H.; Geller-Rhomberg, S.; Stark, N.; Winder, T.; Geiger, K.; Muendlein, A. Optimized allele-specific real-

time PCR assays for the detection of common mutations in KRAS and BRAF. *J. Mol. Diagn.* **2011**, *13*, 23–28.

(11) Yang, Z.; Zhao, N.; Chen, D.; Wei, K.; Su, N.; Huang, J. F.; Xu, H. Q.; Duan, G. J.; Fu, W. L.; Huang, Q. Improved detection of BRAF V600E using allele-specific PCR coupled with external and internal controllers. *Sci. Rep.* **2017**, *7*, 13817.

(12) Siravegna, G.; Marsoni, S.; Siena, S.; Bardelli, A. Integrating liquid biopsies into the management of cancer. *Nat. Rev. Clin. Oncol.* **2017**, *14*, 531–548.

(13) Wang, Q.; Yang, L.; Yang, X.; Wang, K.; He, L.; Zhu, J. Electrochemical biosensors for detection of point mutation based on surface ligation reaction and oligonucleotides modified gold nanoparticles. *Anal. Chim. Acta* **2011**, *688*, 163–167.

(14) Nur Topkaya, S.; Kosova, B.; Ozsoz, M. Detection of Janus Kinase 2 gene single point mutation in real samples with electrochemical DNA biosensor. *Clin. Chim. Acta* **2014**, *429*, 134–139.

(15) Zeng, N.; Xiang, J. Detection of KRAS G12D point mutation level by anchor-like DNA electrochemical biosensor. *Talanta* **2019**, *198*, 111–117.

(16) Sierpe, R.; Kogan, M. J.; Bollo, S. Label-free oligonucleotide-based spr biosensor for the detection of the gene mutation causing prothrombin-related thrombophilia. *Sensors* **2020**, *20*, 6240.

(17) Nguyen, A. H.; Sim, S. J. Nanoplasmonic biosensor: Detection and amplification of dual bio-signatures of circulating tumor DNA. *Biosens. Bioelectron.* **2015**, *67*, 443–449.

(18) Papadakis, G.; Gizeli, E. Screening for mutations in BRCA1 and BRCA2 genes by measuring the acoustic ratio with QCM. *Anal. Methods* **2014**, *6*, 363–371.

(19) Papadakis, G.; Tsortos, A.; Kordas, A.; Tiniakou, I.; Morou, E.; Vontas, J.; Kardassis, D.; Gizeli, E. Acoustic detection of DNA conformation in genetic assays combined with PCR. *Sci. Rep.* **2013**, *3*, 2033.

(20) Dell'Atti, D.; Tombelli, S.; Minunni, M.; Mascini, M. Detection of clinically relevant point mutations by a novel piezoelectric biosensor. *Biosens. Bioelectron.* **2006**, *21*, 1876–1879.

(21) Xu, Q.; Chang, K.; Lu, W.; Chen, W.; Ding, Y.; Jia, S.; Zhang, K.; Li, F.; Shi, J.; Cao, L.; et al. Detection of single-nucleotide polymorphisms with novel leaky surface acoustic wave biosensors, DNA ligation and enzymatic signal amplification. *Biosens. Bioelectron.* **2012**, *33*, 274–278.

(22) Bellasai, N.; Spoto, G. Biosensors for liquid biopsy: circulating nucleic acids to diagnose and treat cancer. *Anal. Bioanal. Chem.* **2016**, *408*, 7255–7264.

(23) Das, J.; Ivanov, I.; Sargent, E. H.; Kelley, S. O. DNA Clutch Probes for Circulating Tumor DNA Analysis. *J. Am. Chem. Soc.* **2016**, *138*, 11009–11016.

(24) D'Agata, R.; Bellasai, N.; Allegretti, M.; Rozzi, A.; Korom, S.; Manicardi, A.; Melucci, E.; Pescarmona, E.; Corradini, R.; Giacomini, P.; et al. Direct plasmonic detection of circulating RAS mutated DNA in colorectal cancer patients. *Biosens. Bioelectron.* **2020**, *170*, 112648.

(25) Kiriimli, C.; Lin, S.; Su, Y.-H.; Shih, W.-H.; Shih, W. Y. In situ, amplification-free double-stranded mutation detection at 60 copies/ml with thousand-fold wild type in urine. *Biosens. Bioelectron.* **2018**, *119*, 221–229.

(26) Alix-Panabières, C. The future of liquid biopsy. *Nature* **2020**, *579*, S9.

(27) Zaman, A.; Wu, W.; Bivona, T. G. Targeting oncogenic braf: Past, present, and future. *Cancers* **2019**, *11*, 1197.

(28) Merz, V.; Gaule, M.; Zecchetto, C.; Cavaliere, A.; Casalino, S.; Pesoni, C.; Contarelli, S.; Sabbadini, F.; Bertolini, M.; Mangiameli, D.; et al. Targeting KRAS: The Elephant in the Room of Epithelial Cancers. *Front. Oncol.* **2021**, *11*, 638360.

(29) Reimhult, E.; Höök, F.; Kasemo, B. Intact vesicle adsorption and supported biomembrane formation from vesicles in solution: Influence of surface chemistry, vesicle size, temperature, and osmotic pressure. *Langmuir* **2003**, *19*, 1681–1691.

(30) Melzak, K. A.; Bender, F.; Tsortos, A.; Gizeli, E. Probing mechanical properties of liposomes using acoustic sensors. *Langmuir* **2008**, *24*, 9172–9180.

(31) Frisken, B. J.; Asman, C.; Patty, P. J. Studies of vesicle extrusion. *Langmuir* **2000**, *16*, 928–933.

(32) Gillissen, J. J. J.; Jackman, J. A.; Tabaei, S. R.; Cho, N.-J. A Numerical Study on the Effect of Particle Surface Coverage on the Quartz Crystal Microbalance Response. *Anal. Chem.* **2018**, *90*, 2238–2245.

(33) Michaelidou, K.; Koutoulaki, C.; Mavridis, K.; Vorrias, E.; Papadaki, M. A.; Koutsopoulos, A. V.; Mavroudis, D.; Agelaki, S. Detection of KRAS G12/G13 Mutations in Cell Free-DNA by Droplet Digital PCR, Offers Prognostic Information for Patients with Advanced Non-Small Cell Lung Cancer. *Cells* **2020**, *9*, 2514.

(34) Abd-El salam, K. A. Bioinformatic tools and guideline for PCR primer design. *Afr. J. Biotechnol.* **2003**, *2*, 91–95.

(35) Mouliere, F.; Chandrananda, D.; Piskorz, A. M.; Moore, E. K.; Morris, J.; Ahlborn, L. B.; Mair, R.; Goranova, T.; Marass, F.; Heider, K.; et al. Enhanced detection of circulating tumor DNA by fragment size analysis. *Sci. Transl. Med.* **2018**, *10*, No. eaat4921.

(36) Grammoustianou, A.; Papadakis, G.; Gizeli, E. Solid-Phase Isothermal DNA Amplification and Detection on Quartz Crystal Microbalance Using Liposomes and Dissipation Monitoring. *IEEE Sensors Lett.* **2017**, *1*, 1–4.

(37) Patolsky, F.; Lichtenstein, A.; Willner, I.; October, R. V. Electronic Transduction of DNA Sensing Processes on Surfaces: Amplification of DNA Detection and Analysis of Single-Base Mismatches by Tagged Liposomes. *Am. Chem. Soc.* **2001**, *123*, 5194–5205.

(38) Patolsky, F.; Lichtenstein, A.; Willner, I.; August, R. V. Amplified Microgravimetric Quartz-Crystal-Microbalance Assay of DNA Using Oligonucleotide-Functionalized Liposomes or Biotinylated Liposomes. *J. Am. Chem. Soc.* **2000**, *122*, 418–419.

(39) Milioni, D.; Mateos-Gil, P.; Papadakis, G.; Tsortos, A.; Sarlidou, O.; Gizeli, E. Acoustic Methodology for Selecting Highly Dissipative Probes for Ultrasensitive DNA Detection. *Anal. Chem.* **2020**, *92*, 8186–8193.

(40) Mitsakakis, K.; Gizeli, E. Multi-sample acoustic biosensing microsystem for protein interaction analysis. *Biosens. Bioelectron.* **2011**, *26*, 4579–4584.

(41) Fernandez, R.; Calero, M.; Reviakine, I.; Garcia-Narbon, J. V.; Rocha-Gaso, M. I.; Arnau, A.; Jimenez, Y. High Fundamental Frequency (HFF) Monolithic Resonator Arrays for Biosensing Applications: Design, Simulations, and Experimental Characterization. *IEEE Sens. J.* **2021**, *21*, 284–295.

(42) Mitsakakis, K.; Tsortos, A.; Gizeli, E. Quantitative determination of protein molecular weight with an acoustic sensor; significance of specific versus non-specific binding. *Analyst* **2014**, *139*, 3918–3925.

(43) Reviakine, I.; Johannsmann, D.; Richter, R. P. Hearing what you cannot see and visualizing what you hear: interpreting quartz crystal microbalance data from solvated interfaces. *Anal. Chem.* **2011**, *83*, 8838–8848.

(44) Raptis, V.; Tsortos, A.; Gizeli, E. Theoretical Aspects of a Discrete-Binding Approach in Quartz-Crystal Microbalance Acoustic Biosensing. *Phys. Rev. Appl.* **2019**, *11*, 034031.

(45) Vázquez-quesada, A.; Schofield, M. M.; Tsortos, A.; Mateos-gil, P.; Milioni, D.; Gizeli, E.; Delgado-buscalioni, R. Hydrodynamics of Quartz-Crystal-Microbalance DNA Sensors Based on Liposome Amplifiers. *Phys. Rev. Appl.* **2020**, *13*, 064059.

(46) Tsortos, A.; Papadakis, G.; Mitsakakis, K.; Melzak, K. A.; Gizeli, E. Quantitative determination of size and shape of surface-bound DNA using an acoustic wave sensor. *Biophys. J.* **2008**, *94*, 2706–2715.

(47) Papadakis, G.; Tsortos, A.; Gizeli, E. Acoustic characterization of nanoswitch structures: Application to the DNA holliday junction. *Nano Lett.* **2010**, *10*, 5093–5097.

(48) Tsortos, A.; Papadakis, G.; Gizeli, E. On the Hydrodynamic Nature of DNA Acoustic Sensing. *Anal. Chem.* **2016**, *88*, 6472–6478.

(49) Tsortos, A.; Grammoustianou, A.; Lymbouridou, R.; Papadakis, G.; Gizeli, E. Detection of multiple DNA targets with a single probe using a conformation-sensitive acoustic sensor. *Chem. Commun.* **2015**, *51*, 11504–11507.

(50) Wang, H.; Jiang, J.; Mostert, B.; Sieuwerts, A.; Martens, J. W. M.; Sleijfer, S.; Foekens, J. A.; Wang, Y. Allele-specific, non-extendable primer blocker PCR (AS-NEPB-PCR) for DNA mutation detection in cancer. *J. Mol. Diagn.* **2013**, *15*, 62–69.

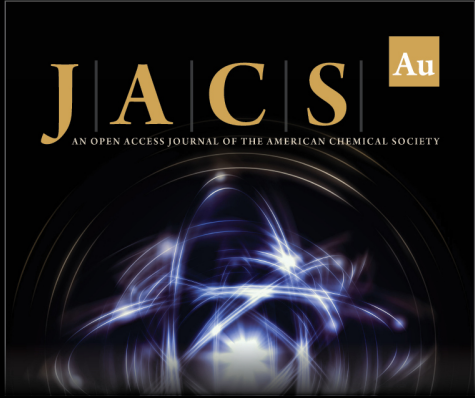
(51) Barbano, R.; Pasculli, B.; Coco, M.; Fontana, A.; Copetti, M.; Rendina, M.; Valori, V. M.; Graziano, P.; Maiello, E.; Fazio, V. M.; et al. Competitive allele-specific TaqMan PCR (Cast-PCR) is a sensitive, specific and fast method for BRAF V600 mutation detection in Melanoma patients. *Sci. Rep.* **2015**, *5*, 18592.

(52) Lade-Keller, J.; Rømer, K. M.; Guldberg, P.; Riber-Hansen, R.; Hansen, L. L.; Steiniche, T.; Hager, H.; Kristensen, L. S. Evaluation of BRAF mutation testing methodologies in formalin-fixed, paraffin-embedded cutaneous melanomas. *J. Mol. Diagn.* **2013**, *15*, 70–80.


(53) Aung, K. L.; Donald, E.; Ellison, G.; Bujac, S.; Fletcher, L.; Cantarini, M.; Brady, G.; Orr, M.; Clack, G.; Ranson, M.; et al. Analytical validation of BRAF mutation testing from circulating free DNA using the amplification refractory mutation testing system. *J. Mol. Diagn.* **2014**, *16*, 343–349.


(54) Ji Eun, O.; Hee Sun, L.; Chang Hyeok, A.; Eun Goo, J.; Ji Youn, H.; Sug Hyung, L.; Nam Jin, Y. Detection of low-level KRAS mutations using PNA-mediated asymmetric PCR clamping and melting curve analysis with unlabeled probes. *J. Mol. Diagn.* **2010**, *12*, 418–424.


(55) Watanabe, K.; Fukuhara, T.; Tsukita, Y.; Morita, M.; Suzuki, A.; Tanaka, N.; Terasaki, H.; Nukiwa, T.; Maemondo, M. EGFR Mutation Analysis of Circulating Tumor DNA Using an Improved PNA-LNA PCR Clamp Method. *Can. Respir. J.* **2016**, *2016*, 5297329.



JACS Au
AN OPEN ACCESS JOURNAL OF THE AMERICAN CHEMICAL SOCIETY

 Editor-in-Chief
Prof. Christopher W. Jones
Georgia Institute of Technology, USA

Open for Submissions 

pubs.acs.org/jacsau  ACS Publications
Most Trusted. Most Cited. Most Read.